IEEJ Journal of Industry Applications
Vol.7 No.3 pp.236–243 DOI: 10.1541/ieejjia.7.236

Paper

Spatial Disturbance Suppression of a Flexible System Based on Wave Model

Yuuki Inoue* Student Member, Seiichiro Katsura* Senior Member

(Manuscript received May 1, 2017, revised Oct. 9, 2017)

Currently, there is a need for precise motion control of industrial machines. For precise motion, it is important to keep the motion robust against disturbances such as gravity or reaction force from the environment. Industrial machines include flexible components such as gears and couplings, and they are modeled as a resonant system. Models expressing resonant systems are classified into lumped-parameter model and distributed-parameter model. Conventionally, the control theory based on the lumped-parameter model has been widely researched because that model is easy to deal with. However, the position which a disturbance acts on is limited to the generator or the lumped inertia of the load in these methods. Therefore, there is a danger that the disturbance suppression performance may deteriorate in the case that a distributed disturbance acts on the load. Here, the distributed-parameter model considering the position which a disturbance acts on, is proposed based on the wave equation. Wave-based modeling can consider the spatial dynamics of a disturbance. As a result, conventional disturbance suppression control is extended for the spatial dynamics.

Keywords: robust control, vibration control, wave system, reflected wave rejection, spatial disturbance

1. Introduction

Recently, high-speed and high-precise control of industrial machines such as industrial robots has been needed to produce high quality and low-cost industrial products [1][2]. It is necessary to drive these machines robustly against disturbances such as gravity or reaction force caused by an environment [3]. Therefore the robust control against disturbance has been researched for a long time [4][5].

Generally, industrial machines include many flexible elements such as gears and couplings [6]. These machines are modeled as a resonant system in control system design [7][8]. Models of resonant system are divided into two types [9]. One is the lumped-parameter model and the other is the distributed-parameter model [10][11]. In the industrial fields, the lumped-parameter model is often utilized because the model is simple and it is easy to deal with [12][13]. Therefore, the control theory based on the lumped-parameter model has been widely researched [14][15]. Particularly, the robust control theory against disturbance acting on the load in the lumped-parameter model has advanced [16].

However, the position which a disturbance acts on is limited in the conventional disturbance suppression control based on the lumped-parameter model. Specifically, the position which a disturbance acts on is limited to the generator such as the motor or the lumped inertia of the load. Therefore, there is a danger that the performance of the disturbance estimation and suppression deteriorates in the case that the position which a disturbance acts on is different from the position of the inertia in the model, or the case that a distributed disturbance acts on the load. It is necessary to utilize high order multi-mass system to improve the performance of the disturbance estimation. However, the model becomes complicated thereby and the control design becomes difficult.

Hence, this paper proposes the distributed-parameter model that is considering the position that a disturbance acting on to express the dynamics of the resonance system. Based on the distributed-parameter model, the robust control against a disturbance which has the spatial dynamics is achieved. By using the distributed-parameter model, a disturbance including the spatial characteristics can be modeled because it is possible to take the spatial dynamics into account in the distributed-parameter model. In this way, the case that a distributed disturbance acts on the load can be deal with. As a result, the conventional disturbance suppression control is extended regarding the spatial dynamics.

In this paper, the wave system is utilized as a distributed-parameter model [9][17]. The wave system is expressed by the wave equation [18][19]. The dynamics of the wave system is described by the time delay element and it is possible to design a simpler control system than the conventional multi-mass system [20]. The vibration suppression control is important to achieve high-speed and precise motion control [21]. In the wave system, vibration suppression is achieved by the rejection of the reflected wave in a plant [9][22].

Thus, a disturbance that has the spatial dynamics is defined as a spatial disturbance in this paper and the control design for the estimation and suppression of a spatial disturbance is conducted. Firstly, the wave system which a spatial disturbance acts on is derived. Secondly, the reflected wave rejection, which is the effective vibration suppression technique in the resonant system, is implemented. Thirdly, a controller for the estimation and suppression of the disturbance is proposed. Finally, the validity of the proposed control system is verified through experiments.

* Department of System Design Engineering Keio University
3-14-1, Hiyoshi, Kohoku-ku, Yokohama 223-8522, Japan

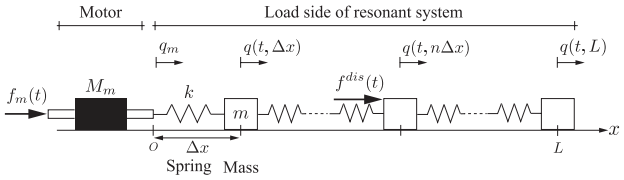

Fig. 1. Model of a multi-mass resonant system considering spatial disturbance

2. Modeling of Wave System Considering Spatial Disturbance

In this section, the wave system under the consideration of a spatial disturbance is modeled. Next, the disturbance observer is implemented in the generator to suppress disturbances which act on the generator side [23][24]. The wave system considering a spatial disturbance is derived by taking the limit of the number of mass in the multi-mass system to infinity. The multi-mass system is shown in Fig. 1. In Fig. 1, t, x, Δx, n, L, $f_m(t)$, $f^{dis}(t)$, M_m, $\bigcirc_m$, q, k, m denote the time, the spatial coordinate, the length of the spring, nth mass, the entire length of the load side of a multi-mass system, the force generated by the motor, disturbance acting on the load side, the inertia of the motor, a variable of the motor, the position of a mass, the spring coefficient, the inertia of a mass, respectively. The multi-mass system is composed of the motor and masses of the load side and each mass is connected by springs.

The motion equation of each mass is expressed as

$$\begin{aligned} M_m\ddot{q}_m &= f_m(t) - k(q_m - q(t,\Delta x)) \\ &\vdots \\ m\ddot{q}(t,n\Delta x) &= k(q(t,(n+1)\Delta x) \\ &\quad -2q(t,n\Delta x) + q(t,(n-1)\Delta x)) \\ &\quad +f^{dis}(t)\left(u(x-x^{dis}) - u(x-(x^{dis}+\Delta x))\right) \\ &\vdots \\ m\ddot{q}(t,N\Delta x) &= -k(q(t,N\Delta x) - q(t,(N-1)\Delta x)), \cdots (1) \end{aligned}$$

where u and x^{dis} denote the step function and the coordinate which disturbance acts on. Here, the boundary conditions are expressed as

$$\begin{aligned} -k(q_m - q(t,\Delta x)) &= M_m\ddot{q}_m - f_m(t) \\ -k(q(t,N\Delta x) - q(t,(N+1)\Delta x)) &= 0. \cdots\cdots (2) \end{aligned}$$

Then, a wave equation is derived by taking the limit of the number of mass to infinity. Specifically, after dividing by Δx in motion equations except those at boundaries (1), $N \to \infty$ and $\Delta x \to 0$ are conducted in (1) and (2). In these conditions, each variable is transformed as

$$\begin{aligned} &\rho = \lim_{\Delta x\to 0}\frac{m}{\Delta x},\ \kappa = \lim_{\Delta x\to 0} k\Delta x,\ x = \lim_{\substack{\Delta x\to 0\\ n\to\infty}} n\Delta x,\ c = \sqrt{\frac{\kappa}{\rho}} \\ &\delta(x-x^{dis}) = \lim_{\Delta x\to 0}\frac{u(x-x^{dis}) - u(x-(x^{dis}+\Delta x))}{\Delta x}, \\ &\qquad\qquad\qquad\qquad\qquad\qquad \cdots\cdots (3) \end{aligned}$$

where ρ, κ, c and δ denote the linear density, the spring coefficient per unit length, the propagation velocity of waves and the delta function. Accordingly, the wave equation is derived from (1) as

$$\frac{\partial^2 q(t,x)}{\partial t^2} = c^2\frac{\partial^2 q(t,x)}{\partial x^2} + \frac{1}{\rho}f^{dis}(t)\delta(x-x^{dis}). \cdots\cdots (4)$$

In this paper, the resonant system described by the wave equation is called the wave system. The disturbance observer is implemented to the motor, then the boundary conditions of the resonance system are derived from (2) as

$$\begin{aligned} &q(t,0) = q_m \\ &\frac{\partial q(t,L)}{\partial x} = 0. \cdots\cdots (5) \end{aligned}$$

Then, the transfer function of the wave system is derived. The initial conditions of the wave system are set as

$$\begin{aligned} &q(0,x) = 0 \\ &\frac{\partial q(0,x)}{\partial t} = 0. \cdots\cdots (6) \end{aligned}$$

By applying Laplace transformation, the boundary conditions (5) and the initial conditions (6) to (4), the position of the load is derived as

$$\begin{aligned} Q(s,x) = &\frac{e^{-\frac{2L-x}{c}s} + e^{-\frac{x}{c}s}}{1+e^{-\frac{2L}{c}s}}Q_m + \frac{1}{\sqrt{\rho\kappa}s}\frac{e^{-\frac{L-x}{c}s} - e^{-\frac{L+x}{c}s}}{1+e^{-\frac{2L}{c}s}}F^{dis}(s) \\ &-\frac{1}{\kappa}F^{dis}(s)r(x-x^{dis}), \cdots\cdots (7) \end{aligned}$$

where s, Q, F^{dis} and r denote the Laplace operator, the position in Laplace domain, disturbance in Laplace domain and the ramp function respectively. By substitute $x = L$ in (7), the tip position of the load is derived as

$$\begin{aligned} Q(s,L) = &\frac{2e^{-\frac{L}{c}s}}{1+e^{-\frac{2L}{c}s}}Q_m + \frac{1}{\sqrt{\rho\kappa}s}\frac{1-e^{-\frac{2L}{c}s}}{1+e^{-\frac{2L}{c}s}}F^{dis}(s) \\ &-\frac{1}{\kappa}F^{dis}(s)(L-x^{dis}). \cdots\cdots (8) \end{aligned}$$

The wave system is shown in Fig. 2. In Fig. 2, $\ddot{Q}^{ref}$ denote the acceleration reference. As shown in Fig. 2, the spatial dynamics of a disturbance is expressed by the proposed model. In the wave system, waves are expressed as time delay elements.

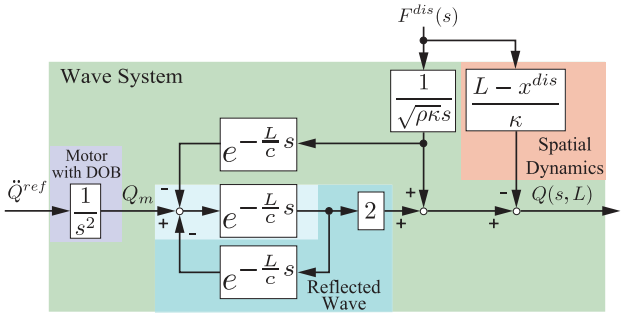

Fig. 2. Wave system considering spatial disturbance

3. Reflected Wave Rejection, Disturbance Estimation and Disturbance Suppression

In this section, the vibration control method called the reflected wave rejection is implemented in the wave system. By the implementation of the reflected wave rejection, the wavesystem is transformed into the mere time delay element.

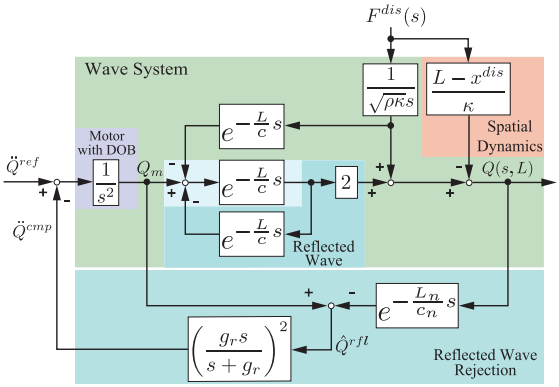

Fig. 3. Reflected wave rejection in wave system

After that, a controller for the estimation and suppression of the spatial disturbance is proposed. In the disturbance suppression control, it is shown that the controller is equivalent to the wave-based disturbance observer that was already proposed [22]. Finally, the whole control system is derived by the combination of the reflected wave rejection and the controller for the estimation and suppression of the spatial disturbance.

3.1 Reflected Wave Rejection The wave system is one of the resonance system and has resonances. In the wave system, a superposition of the traveling wave and the reflected wave causes vibration. Therefore, the reflected wave rejection is effective to suppress vibration [9].

The reflected wave Q^{rfl} in wave system is defined as

$$Q^{rfl} = Q_m - e^{-\frac{L}{c}s}Q(s,L). \cdots (9)$$

Here, the 1st resonant frequency ω_1 is expressed as

$$\omega_1 = \frac{c}{2L}\pi. \cdots (10)$$

In (10), L/c is derived by the identification of ω_1 and (9) can be implemented. Vibration caused from the acceleration reference to the tip position of load is suppressed based on the reflected wave rejection as shown in Fig. 3. However, a disturbance acting on the tip position should be eliminated by other controllers.

3.2 Disturbance Estimation and Disturbance Suppression The estimation and suppression of a disturbance is needed to remain the system robust. The robustness of the motor is guaranteed by the disturbance observer. On the other hand, the robustness of the tip of the load is achieved by the wave-based disturbance observer [22].

First, the load disturbance is defined. (8) is transformed as

$$\left(1+e^{-\frac{2L}{c}s}\right)Q(s,L) = 2e^{-\frac{L}{c}s}Q_m + \left(\frac{1}{\sqrt{\rho\kappa}s}\left(1-e^{-\frac{2L}{c}s}\right) - \frac{L-x^{dis}}{\kappa}\left(1+e^{-\frac{2L}{c}s}\right)\right)F^{dis}(s). \cdots (11)$$

In (11), the load disturbance Q_l^{dis} is defined as

$$Q_l^{dis} = \left(-\frac{1}{\sqrt{\rho\kappa}s}\left(1-e^{-\frac{2L}{c}s}\right)+\frac{L-x^{dis}}{\kappa}\left(1+e^{-\frac{2L}{c}s}\right)\right)F^{dis}(s). \cdots (12)$$

In this paper, disturbance $F^{dis}(s)$ is assumed as a step force.

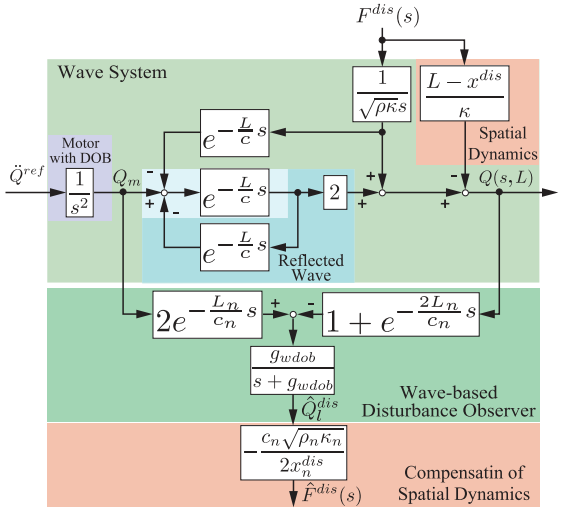

Fig. 4. Estimation of spatial disturbance

The validity of the assumption that disturbance has is a step force is supposed in the end of the subsection. The time delay element in (12) is expanded by the Taylor expansion and (12) is transformed into

$$\begin{aligned} Q_l^{dis} &= -\frac{\frac{2L}{c} - \frac{1}{2}\left(-\frac{2L}{c}\right)^2 s\cdots}{\sqrt{\rho\kappa}}F^{dis}(s) \\ &\quad + \frac{\left(L-x^{dis}\right)\left(2-\frac{2L}{c}s+\cdots\right)}{\kappa}F^{dis}(s) \\ &\approx -\frac{\frac{2L}{c}}{\sqrt{\rho\kappa}}F^{dis}(s) + \frac{L-x^{dis}}{\kappa}2F^{dis}(s) \\ &= -\frac{2x^{dis}}{c\sqrt{\rho\kappa}}F^{dis}(s). \cdots (13) \end{aligned}$$

Then, the spatial disturbance is derived as

$$F^{dis}(s) = -\frac{c\sqrt{\rho\kappa}}{2x^{dis}}Q_l^{dis}. \cdots (14)$$

Whereas, the load disturbance is expressed based on (11) and (12) as

$$Q_l^{dis} = 2e^{-\frac{L}{c}s}Q_m - \left(1+e^{-\frac{2L}{c}s}\right)Q(s,L). \cdots (15)$$

Hence, the load disturbance is estimated as

$$\hat{Q}_l^{dis} = \frac{g_{\mathrm{wdob}}}{s+g_{\mathrm{wdob}}}\left(2e^{-\frac{L_n}{c_n}s}Q_m - \left(1+e^{-\frac{2L_n}{c_n}s}\right)Q(s,L)\right), \cdots (16)$$

where $\hat{\bigcirc}$ and g_{wdob} denote the estimated value and the cut-off frequency of the low pass filter to reduce the influence of the sensor noise, respectively. Load disturbance suppression and the estimation of the spatial disturbance are accomplished based on (14) and (16) as shown in Fig. 4. In Fig. 4, disturbance suppression is achieved by the wave-based disturbance observer which was proposed previously. On the other hand, estimation of the spatial disturbance is conducted by the compensation of the spatial dynamics. The validity of the assumption about disturbance is supposed as follows. In (13), the Taylor expansion is used and infinite number of Taylor expansion terms are approximated by zero-order because

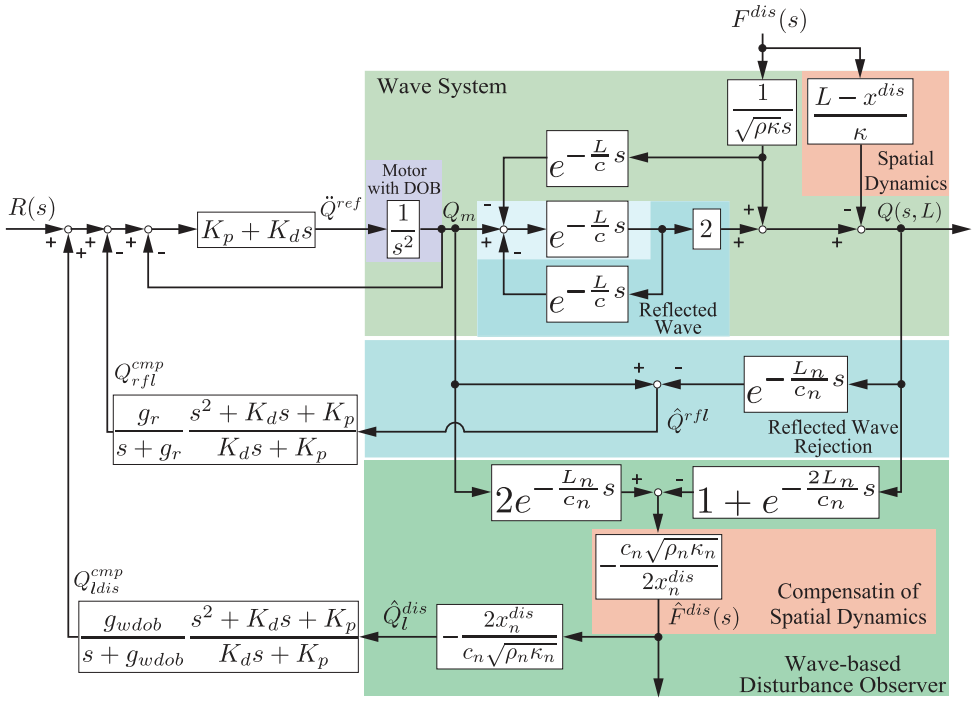

Fig. 5. Whole control system

disturbance $F^{dis}(s)$ is assumed to first-order and it is obvious from the final value theorem that terms having first or more order are not related to the steady-state error. If the better performance of disturbance estimation and disturbance suppression in transient response is desired, it is only necessary to increase the order of approximation in Taylor expansion. In addition, even if the disturbance is expressed as a higher-order force, it can be dealt with by increasing the order of approximation in Taylor expansion. Increasing the order of approximation in Taylor expansion brings high-order term in (14). However, it can be treated by same or higher order filter in wave-based disturbance observer. Therefore, the assumption that disturbance is step force doesn't compromise generality.

Wave-based disturbance observer shown in Fig. 4 has already been proposed in previous researches [22]. However, the position which disturbance acts on is limited to tip of load in the conventional wave-based disturbance observer. In flexible structure, it is needed to consider the position disturbance acting on because influence of disturbance varies by disturbance acting point. In this research, disturbance acting point is considered in observer shown in Fig. 4 as compensation of spatial dynamics and it is possible to estimate spatial disturbance. Therefore, force control and hybrid control based on spatial disturbance will be achieved by proposed observer and these researches will be conducted in future. On the other hand, it may be possible to estimate spatial disturbance acting on flexible structure by application of other lumped [19] or distributed-parameter model based observer [25][26]. However, the control structure will be complex because models using in observer are very intricate. In proposed method, the control structure shown in Fig. 4 is simple and physical meaning of each parameters are understandable. Therefore, it is easy to tune control parameters and implementation isn't difficult. In this way, proposed observer has an advantage in the simplicity of control structure.

3.3 Whole Control System By the proposed method, the transfer function from the motor position to the tip position is derived as

$$\frac{Q(s,L)}{Q_m}=\frac{\frac{g_{\mathrm{wdob}}}{s+g_{\mathrm{wdob}}}e^{-\frac{L_n}{c_n}s}+\left(\frac{g_{\mathrm{wdob}}}{s+g_{\mathrm{wdob}}}e^{-\frac{L_n}{c_n}s}-\left(\frac{g_{\mathrm{r}}}{s+g_{\mathrm{r}}}\right)^2e^{-\frac{L}{c}s}\right)}{\frac{g_{\mathrm{wdob}}}{s+g_{\mathrm{wdob}}}+\left(\frac{g_{\mathrm{wdob}}}{s+g_{\mathrm{wdob}}}e^{-\frac{L_n}{c_n}s}-\left(\frac{g_{\mathrm{r}}}{s+g_{\mathrm{r}}}\right)^2e^{-\frac{L}{c}s}\right)e^{-\frac{L_n}{c_n}s}}. \quad \cdots\cdots\cdots\cdots\cdots (17)$$

As shown in (17), vibration suppression and disturbance suppression is achieved when the reflected wave rejection works enough ($g_{\mathrm{r}} \to \infty$), the wave-based disturbance observer works enough ($g_{\mathrm{wdob}} \to \infty$) and the nominal parameter of the propagation time of wave equals the real parameter ($L_n/c_n = L/c$).

The whole control system in which the proportional-derivative controller is implemented as a position controller is shown in Fig. 5. In Fig. 5, $R(s)$, Q_{rfl}^{cmp}, Q_{ldis}^{cmp}, K_p and K_d denote the position command, the compensation value generated in the reflected wave rejection controller, the compensation value generated in the wave-based disturbance observer, the proportional gain and the derivative gain, respectively. Disturbance suppression performance of the semi closed loop control system against disturbance acting on the motor is better than one of the full closed loop control system. Therefore, the semi closed loop control system is composed in this paper.

4. Analysis of Control System

Analysis of stability, fast response and robustness is conducted through open-loop transfer function, sensitivity function and complementary sensitivity function. In Fig. 5, open-loop transfer function $G_{\mathrm{o}}^{\mathrm{pro}}$ is derived as

Table 1. Parameters in analysis

Parameter	Description	Value
ω_1	1st resonant frequency	133 rad/s
$\frac{L_n}{c_n}$	Propagation time of wave	0.0118 s
M_a	Mass of the load	8.00×10^{-4} kg m^2
K_f	Spring coefficient	5.75 N m
K_p	Position gain	3000
K_d	Velocity gain	110
K_r	Reaction gain	$\frac{4}{M_{an}}$
g_{pse}	Cut-off frequency in PD controller	3000 rad/s

$$G_o^{pro} = \frac{G_w\left(L_w(1+e^{-\frac{2L_n}{c_n}s}) - L_r e^{-\frac{L_n}{c_n}s}\right)}{1+L_r-2L_w e^{-\frac{L_n}{c_n}s}}, \quad \cdots\cdots (18)$$

where G_w, L_r, L_w and $\bigcirc_n$ denote plant expressed by wave equation, low-pass filter in vibration suppression controller, low-pass filter in disturbance suppression controller and nominal value as shown

$$G_w = \frac{2e^{-\frac{L}{c}s}}{1+e^{-\frac{2L}{c}s}}, \quad \cdots\cdots (19)$$

$$L_r = \frac{g_r}{s+g_r}, \quad \cdots\cdots (20)$$

$$L_w = \frac{g_{wdob}}{s+g_{wdob}}. \quad \cdots\cdots (21)$$

For the comparison, control system based on resonance ratio control and load disturbance observer is used as conventional method in this section [27][28]. In the conventional method, open-loop transfer function G_o^{con} is derived as

$$G_o^{con} = \frac{L_w^2 G_w G_m M_{an} s^2\left(\frac{1}{K_f}+\frac{K_r}{K_p}\right)}{1+L_r G_m K_f(1-G_w)\left(\frac{K_r}{K_p}-\left(\frac{1}{K_f}+\frac{K_r}{K_p}\right)L_w^2\right)}. \quad \cdots\cdots (22)$$

where G_m, K_f, K_r, K_p and M_a denote motor with motor position controller and DOB, spring coefficient of plant, reaction force gain in vibration suppression controller, position gain in motor position controller and mass of load. From (18) and (22), stability analysis is conducted through gain margin and phase margin. Then, analysis of fast response is conducted through gain crossover frequency and phase crossover frequency calculated from (18) and (22). In addition, sensitivity function and complementary sensitivity function are calculated from (18) and (22). Then, disturbance suppression performance and robust stability are analyzed. Parameters in following analysis are set as shown Table 1.

4.1 Analysis of Stability and Fast Response Stability analysis of proposed control system and conventional control system is conducted through gain margin and phase margin of open-loop transfer function in proposed control system G_o^{pro} and conventional control system G_o^{con}. Next, analysis of fast response is conducted through gain crossover frequency and phase crossover frequency. Set of gain margin G_m, phase margin P_m, gain crossover frequency W_{gm} and phase crossover frequency W_{pm} of open-loop transfer function are shown in Table 2. In these tables, ω_1 denotes first-order resonant frequency of plant.

In Table 2, cut-off frequencies in vibration suppression controller g_r and disturbance suppression controller g_{wdob} are set to $50\omega_1$ and $1.0\omega_1$, respectively. As shown in Table 2, gain margin and phase margin in proposed method are bigger than one in conventional method. Therefore, proposed method is superior in the view of stability. Moreover, gain crossover frequency and phase crossover frequency of proposed method are bigger than one in conventional method. Therefore, proposed method is considered to has wider control bandwidth and be also superior in the view of fast response.

Table 2. Stability analysis ($g_r = 50\omega_1$, $g_{wdob} = 1.0\omega_1$)

Method	G_m [dB]	P_m[deg]	W_{gm} [rad/s]	W_{pm} [rad/s]
Pro.	1.59	36.1	244	6027
Con.	0.670	19.3	229	1724

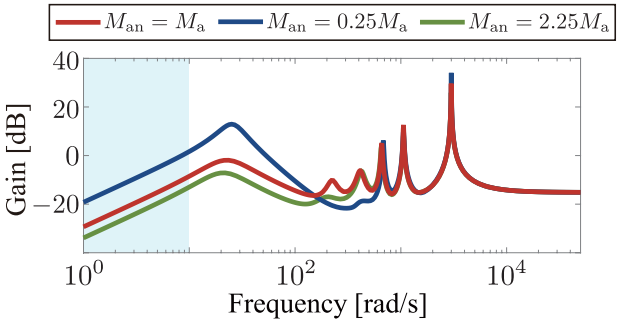

Fig. 6. Sensitivity function in conventional method ($g_r = 50\omega_1$, $g_{wdob} = 1.0\omega_1$)

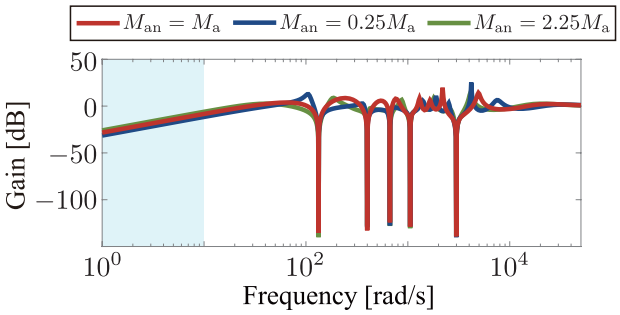

Fig. 7. Sensitivity function in the proposed method ($g_r = 50\omega_1$, $g_{wdob} = 1.0\omega_1$)

4.2 Analysis of Disturbance Suppression Performance Disturbance suppression performance is analyzed through sensitivity function calculated from (18) and (22). Sensitivity functions in conventional method are shown in Fig. 6. Sensitivity functions in proposed method are shown in Fig. 7. In Figs. 6 and 7, cut-off frequencies in vibration suppression controller g_r and disturbance suppression controller g_{wdob} are set to $50\omega_1$ and $1.0\omega_1$, respectively. In Figs. 6 and 7, nominal masses of load M_{an} are set to M_a, $0.25M_a$ and $2.25M_a$. The reason why several mass values are set is to observe the influence of fluctuation of load mass.

As shown in Fig. 6, disturbance suppression performance of conventional method in low frequency band can be seen. However, there are several gain peaks in middle and high frequency band because high-order dynamics such as high-order resonance isn't considered in conventional method. In addition, disturbance suppression performance in low frequency band is largely fluctuated by the fluctuation of load mass and largely degrades in the case that nominal mass

value is smaller than real mass value. On the other hand, disturbance suppression performance of proposed method in low frequency band is better than conventional method as shown in Fig. 7. Disturbance suppression performance in low frequency band isn't so fluctuated by the fluctuation of load mass and disturbance suppression performance is kept. In addition, proposed method is robust against the fluctuation of resonant frequency because gain of sensitivity function around resonant frequency degrades in proposed method. Moreover, there are not so serious gain peaks in middle and high frequency band even if mass of load fluctuates because proposed method considers high-order dynamics of plant. From the above, proposed method is superior to conventional method in the view of disturbance suppression performance.

4.3 Analysis of Robust Stability Robust stability is analyzed through complementary sensitivity function calculated from (18) and (22). Complementary sensitivity functions in conventional method are shown in Fig. 8. Complementary sensitivity functions in proposed method are shown in Fig. 9. In Figs. 8 and 9, cut-off frequencies in vibration suppression controller g_r and disturbance suppression controller g_{wdob} are set to $50\omega_1$ and $1.0\omega_1$, respectively. In Figs. 8 and 9, nominal masses of load M_{an} are set to M_a, $0.25M_a$ and $2.25M_a$.

As shown in Fig. 8, there are some gain peaks in complementary sensitivity function of conventional method. It is serious problem that gain doesn't decrease in high frequency band. Therefore, it can be said that robust stability of conventional method is not desirable. On the other hand, there are also some gain peaks in complementary sensitivity function of proposed method as shown in Fig. 9. However, gain degrades in high frequency band. In addition, the characteristics

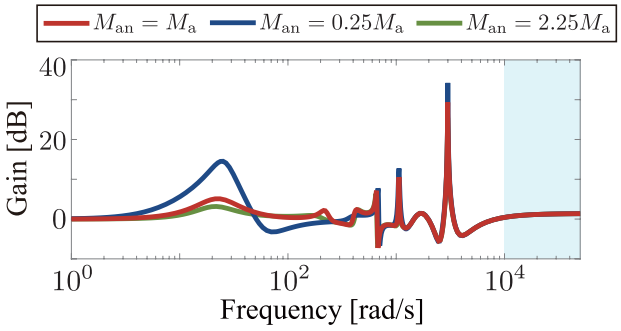

Fig. 8. Complementary sensitivity function in conventional method ($g_r = 50\omega_1$, $g_{wdob} = 1.0\omega_1$)

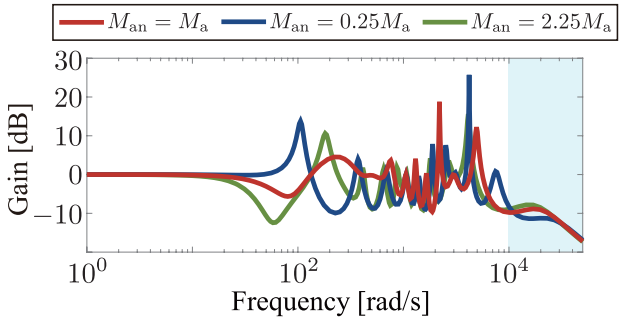

Fig. 9. Complementary sensitivity function in the proposed method ($g_r = 50\omega_1$, $g_{wdob} = 1.0\omega_1$)

that gain decreases in high frequency band can also be seen in the case that mass of load fluctuates. Therefore, it can be said that robust stability of proposed method is largely better than conventional method. In this way, proposed method is superior to conventional method in the view of robust stability.

5. Experiments

5.1 Experimental Setup Experiments of the tip position control were conducted to confirm the effectiveness of the proposed controllers. In experiments, a direct drive motor with a flexible arm was utilized. Flexible arm is assumed to be a load. The motor position was obtained from an encoder (resolution: 20 bit/rev) and the tip position was obtained from a position sensitive detector and laser diode. A step disturbance was applied to the flexible arm by the linear motor at 1.7 s. The control was real-time one based on Linux OS with Real Time Application Interface RTAI 3.7 [29]. The experimental system is shown in Fig. 10. For the comparison, the controller based on the resonance ratio control and the load disturbance observer was utilized as a conventional method 1 [27][28]. In addition, conventional wave-based disturbance observer was also used as a conventional method 2 in the estimation of spatial disturbance. In the position control, disturbance suppression control in the conventional method 2 and proposed method are equivalent. Therefore, position control results were compared between conventional method 1 and proposed method. In experiments of position control, disturbance estimation was also conducted. In estimation of spatial disturbance, conventional method 1 and 2 were compared with proposed method. Parameters of experimental system are shown in Table 3. Control parameters in conventional method are shown in Table 4. Control parameters in proposed method are shown in Table 5. The sampling time was set to 50 μs.

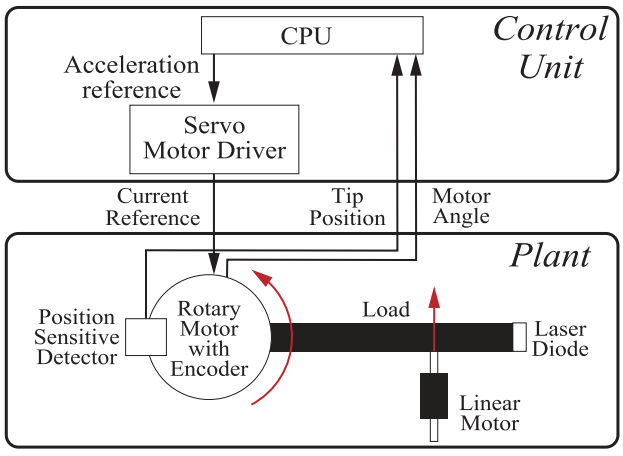

Fig. 10. Experimental system

Table 3. Parameters of experimental system

Parameter	Description	Value
ω_m	1st resonant frequency	133 rad/s
K_t	Torque constant	1.18 Nm/A
M_m	Mass of motor	2.90×10^{-3} kg m^2
L	Length of the load	3.00×10^{-1} m
ρ	Linear density of the load	2.27×10^{-1} kg m^2
x^{dis}	Position which disturbance acts on	$0.7L$

Table 4. Control parameters in conventional method

Parameter	Description	Value
ω_{mn}	Nominal 1st resonant frequency	ω_m
L_n	Nominal length of the load	L
ρ_n	Nominal linear density of the load	ρ
K_p	Position gain	3000
K_d	Velocity gain	110
K_r	reaction force gain	333
g_{pse}	Cut-off frequency in PD controller	3000 rad/s
g_{dis}	Cut-off frequency of DOB	3000 rad/s
g_{rfob}	Cut-off frequency of RFOB	3000 rad/s
g_a	Cut-off frequency of load disturbance observer	40.0 rad/s

Table 5. Control parameters in the proposed method

Parameter	Description	Value
ω_{mn}	Nominal 1st resonant frequency	ω_m
ω_{2mn}	Nominal 2nd resonant frequency	5.50 ω_{mn}
L_n	Nominal length of the load	L
ρ_n	Nominal linear density of the load	ρ
x_n^{dis}	Nominal position which disturbance acts on	x^{dis}
K_p	Position gain	3000
K_d	Velocity gain	110
K_r	reaction force gain	333
g_{pse}	Cut-off frequency in PD controller	3000 rad/s
g_{dis}	Cut-off frequency of DOB	3000 rad/s
g_{rfob}	Cut-off frequency of RFOB	3000 rad/s
g_{wdob}	Cut-off frequency of wave-based disturbance observer	14.4 rad/s

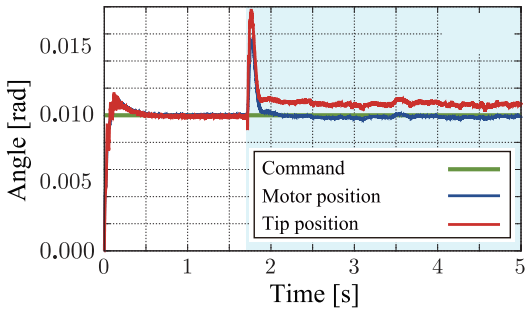

Fig. 11. Experimental results of conventional method 1

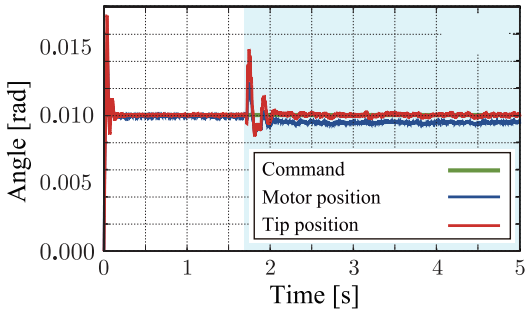

Fig. 12. Experimental results of the proposed method

5.2 Experimental Results Experimental results of tip position control are shown in Figs. 11 and 12. Figure 11 shows the result of the position control in the conventional method 1. Figure 12 shows the result of the position control in the proposed method. As shown in Fig. 11, steady-state error of the tip position occurred in the conventional method by the spatial disturbance. The reason why steady-state error occurred is considered as follows. In the flexible arm utilized in experiments, there is a difference between the spring constant from motor to the tip position and the spring constant from motor to the position which disturbance acts on. Since the spring constant from motor to the position which disturbance

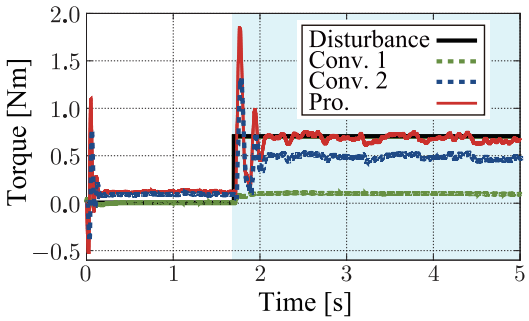

Fig. 13. Experimental results of disturbance estimation

acts on can't be identified in advance, then the spring constant from motor to the tip position was set to nominal value. Similarly, mass of load was set as a value from motor to the tip position in the same way. As a results, these modeling error caused steady-state error. In contrast, as shown in Fig. 12, the tip position was robust against the spatial disturbance and converged the command value in the steady-state. However, the tip position fluctuated in the transient response because wave-based disturbance observer causes vibration. The reason why vibration causes in the beginning of control is considered that damping didn't exist in control system and inverse phase driving was conducted against vibration at high speed after sensing vibration in tip position. In the results of disturbance estimation shown in Fig. 13, conventional method 1 and 2 can't estimate the spatial disturbance because the spatial dynamics wasn't considered in these methods. On the other hand, disturbance was estimated enough in the steady-state by the proposed method. However, estimation value fluctuated in the transient response because of the approximation in (13) and viscous friction. The estimated force didn't match to 0 in the initial-state because of the influence of static friction. Thus, the effectiveness of the proposed method was verified through experiments.

6. Conclusions

A disturbance estimation and suppression control against a disturbance that has the spatial dynamics based on the wave system was proposed. On the model of the resonant system, the position which a disturbance acting on is limited in the conventional lumped-parameter model. Therefore, it is difficult to consider the point a disturbance acting on strictly or the case that a distributed disturbance acts. Hence, the modeling based on the wave system which is a kind of the distributed-parameter model was conducted. In this way, the spatial dynamics of a disturbance could be considered. The reflected wave rejection, which is a vibration control method in the wave system was implemented because the vibration control is needed in the control of the resonant system. Furthermore, the control system for the estimation and suppression of a spatial disturbance was proposed. Here, the control system for a spatial disturbance suppression was equivalent to the wave-based disturbance observer that was already proposed. Finally, the validity of the proposed control system was verified by experiments.

Acknowledgment

This research was partially supported by the Ministry of Internal Affairs and Communications, Strategic

Information and Communications R&D Promotion Programme (SCOPE), 151203009, 2017.

References

(1) M. Iwasaki, K. Seki, and Y. Maeda: "High-precision motion control techniques: A promising approach to improving motion performance", *IEEE Industrial Electronics Magazine*, Vol.6, No.1, pp.32–40 (2012)

(2) T. Oiwa and M. Katsuki: "Survey of questionnaire on ultra-precision positioning", *Journal of the Japan Society for Precision Engineering*, Vol.81, No.10, pp.904–910 (2015)

(3) K. Yamaguchi, M. Hirata, and H. Fujimoto: "Nanoscale servo control", Tokyo Denki University Press (2007)

(4) K. Ohnishi, M. Shibata, and T. Murakami: "Motion control for advanced mechatronics", *IEEE/ASME Transactions on Mechatronics*, Vol.1, No.1, pp.56–67 (1996)

(5) J.N. Yun, J. Su, Y.I. Kim, and Y.C. Kim: "Robust disturbance observer for two-inertia system", *IEEE Transactions on Industrial Electronics*, Vol.60, No.7, pp.2700–2710 (2013)

(6) M. Yang, C. Wang, D. Xu, W. Zheng, and X. Lang: "Shaft torque limiting control using shaft torque compensator for two-inertia elastic system with backlash", *IEEE/ASME Transactions on Mechatronics*, Vol.21, No.6, pp.2902–2911 (2016)

(7) T. Mori, K. Fuwa, and H. Kando: "Vibration control of flexible structures via optimal servo control system using notch filter", *Transactions on the Society of Instrument and Control Engineers*, Vol.44, No.7, pp.611–613 (2008)

(8) M. Aoki, H. Fujimoto, Y. Hori, and T. Takahashi: "Robust resonance suppression control based on self resonance cancellation disturbance observer and application to humanoid robot", 2013 IEEE International Conference on Mechatronics (ICM), pp.623–628 (2013)

(9) E. Saito and S. Katsura: "Vibration control of resonant system by using reflected wave rejection with fractional order low-pass filter", 2013 IEEE International Conference on Mechatronics (ICM), pp.853–858 (2013)

(10) S. H. Song, J.K. Ji, S.K. Sul, and M.H. Park: "Torsional vibration suppression control in 2-mass system by state feedback speed controller", Proceedings of IEEE International Conference on Control and Applications, Vol.1, pp.129–134 (1993)

(11) E. Kreyszig: "Advanced engineering mathematics", *Wiley* (2005)

(12) A. Al-Mamun, E. Keikha, C.S. Bhatia, and T.H. Lee: "Integral resonant control for suppression of micro-actuator resonance in dual stage actuator", *IEEE Trans. Magnetics*, Vol.48, No.11, pp.4614–4617 (2012)

(13) K. Ohno and T. Hara: "Adaptive resonant mode compensation for hard disk drives", *IEEE Transactions on Industrial Electronics*, Vol.53, No.2, pp.624–630 (2006)

(14) S. Morimoto and Y. Takeda: "Two-degrees-of-freedom speed control of resonant mechanical system based on h_∞ control theory", *IEEJ Trans. IA*, Vol.116, No.1, pp.65–70 (1996)

(15) S. Yamada and H. Fujimoto: "Vibration suppression control for a two-inertia system using load-side high-order state variables obtained by a high-resolution encoder", IECON 2014 - 40th Annual Conference of the IEEE Industrial Electronics Society, pp.2897–2903 (2014)

(16) Y. Imaizumi, S. Urushihara, K. Ohishi, and T. Miyazaki: "Design of robust load position servo system for two inertia resonant system based on the estimated load information", *IEEJ Trans. IA*, Vol.130, No.7, pp.847–857 (2010)

(17) Y. Halevi: "Control of flexible structures governed by the wave equation using infinite dimensional transfer functions", ASME Journal of Dynamic Systems, Measurement, and Control, Vol.127, No.4, pp.579–589 (2005)

(18) C. Wagner-Nachshoni, and Y. Halevi: "Control of multi-link flexible structures", Proceedings of the 2005 IEEE International Symposium on, Mediterrean Conference on Control and Automation Intelligent Control, 2005, pp.507–512 (2005)

(19) W.J. O'Connor: "Wave-based analysis and control of lump-modeled flexible robots", *IEEE Trans. Robotics*, Vol.23, No.2, pp.342–352 (2007)

(20) Y. Inoue, E. Saito, and S. Katsura: "Feedforward control design of wave system based on reaction force", The 2nd IEEJ International Workshop on Sensing, Actuation, and Motion Control, and Optimization, SAMCON2016 (2016)

(21) Y. Hori, H. Sawada, and Y. Chun: "Slow resonance ratio control for vibration suppression and disturbance rejection in torsional system", *IEEE Trans. Industrial Electronics*, Vol.46, No.1, pp.162–168 (1999)

(22) E. Saito and S. Katsura: "Position control of resonant system with load force suppression using wave observer", *IEEJ Journal of IA*, Vol.3, No.1, pp.18–25 (2014)

(23) K. Ohishi, K. Ohnishi, and M. Miyachi: "Torque-speed regulation of dc motor based on load torque estimation method", Proc. Int. Power Electron. Conf., pp.1209–1218 (1983)

(24) S. Katsura, Y. Matsumoto, and K. Ohnishi: "Modeling of force sensing and validation of disturbance observer for force control", *IEEE Transactions on Industrial Electronics*, Vol.54, No.1, pp.530–538 (2007)

(25) F. Matsuno, S. Kasai, M. Tanaka, and K. Wakashiro: "Robust force control of a one-link flexible arm", *Transactions of the Society of Instrument and Control Engineers*, Vol.32, No.7, pp.1011–1019 (1996)

(26) F. Matsuno and K. Yamamoto: "Dynamic hybrid position/force control of a two-degree-of-freedom flexible manipulator", *Transactions of the Society of Instrument and Control Engineers*, Vol.29, No.6, pp.677–684 (1993)

(27) K. Yuki, T. Murakami, and K. Ohnishi: "Vibration control of 2 mass resonant system by resonance ratio control", Industrial Electronics, Control, and Instrumentation, 1993. Proceedings of the IECON '93., International Conference on, Vol.3, pp.2009–2014 (1993)

(28) M. Matsuoka, T. Murakami, and K. Ohnishi: "Vibration suppression and disturbance rejection control of a flexible link arm", Industrial Electronics, Control, and Instrumentation, 1995. Proceedings of the IECON '95, International Conference on, Vol.2, pp.1260–1265 (1995)

(29) R. Bucher, S. Mannori, and T. Netter. (2008, Feb.) Rtai-lab tutorial: Scilab, comedi, and real time-control. [Online]. Available: https://www.rtai.org/userfiles/downloads/RTAILAB/RTAI-Lab-tutorial.pdf

Yuuki Inoue (Student Member) received the B.E. degree in system design engineering from Keio University, Yokohama, Japan, in 2016. Since 2016, he has been in the Master's course at Keio University, Yokohama, Japan. His research interests include motion control and vibration suppression control. He is a Student Member of IEEJ, as well as a Student Member of the IEEE.

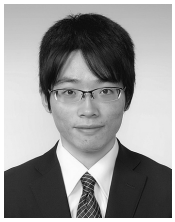

Seiichiro Katsura (Senior Member) received the B.E. degree in system design engineering and the M.E. and Ph.D. degrees in integrated design engineering from Keio University, Yokohama, Japan, in 2001, 2002 and 2004, respectively. From 2003 to 2005, he was a Research Fellow of the Japan Society for the Promotion of Science (JSPS). From 2005 to 2008, he worked at Nagaoka University of Technology, Nagaoka, Niigata, Japan. Since 2008, he has been at Keio University, Yokohama, Japan. In 2017, he was a Visiting Researcher with The Laboratory for Machine Tools and Production Engineering (WZL) of RWTH Aachen University, Aachen, Germany. His research interests include applied abstraction, human support, wave system, systems energy conversion, and electromechanical integration systems. Prof. Katsura serves as an Associate Editor of the IEEE Transactions on Industrial Electronics. He was the recipient of The Institute of Electrical Engineers of Japan (IEEJ) Distinguished Paper Awards in 2003 and 2017, IEEE Industrial Electronics Society Best Conference Paper Award in 2012, and JSPS Prize in 2016.